ELSEVIER

PII S0142-9612(97)00022-7

Biomaterials **18** (1997) 1027–1035

0142-9612/97/$17.00

Formation and characteristics of the apatite layer on plasma-sprayed hydroxyapatite coatings in simulated body fluid

Jie Weng*†, Qing Liu*, J.G.C. Wolke*, Xingdong Zhang† and K. de Groot*

**Biomedical Innovation Group, University of Leiden, Wassenaarseweg 62, Building 4, 2333 AL Leiden, The Netherlands; †Institute of Materials Science and Technology, Sichuan University, Chengdu 610064, P.R. China*

Plasma-sprayed hydroxyapatite (HA) coatings were incubated in simulated body fluids (SBFs) for different periods of time to investigate the nucleation and growth of apatite on their surface. The layer that formed was recognized as having similarities to bone apatite because it is poorly crystallized, non-stoichiometric or calcium deficient, and contains carbonate and magnesium. Scanning electron microscopy (SEM) and infrared spectroscopy (IR) were employed to investigate the morphological changes of the coating surface and the structure of the grown layer respectively. In the first few hours, calcium and phosphate ions dissolved from the coatings so as to increase their local supersaturation to a higher degree, thereafter followed by the nucleation and growth of apatite. The nucleation occurred firstly on the recessed regions, inside pores and cracks where the higher supersaturation was readily maintained. Only after 24 h incubation was a complete layer formed on the surface of the coating. There is no obvious interface between the grown layer and the underlying coating. Heat treatment in the air made the apatite transform into biphasic calcium phosphate of HA and tricalcium phosphate, with a blue colour because of trace manganese ions. The heat-treated HA coating showed no dissolution by SEM observation. This resulted in no precipitation on the surface. When SBF was used with two-fold higher ion concentrations, the apatite layer formed slowly in 72 h without dissolution of the coating surface. This may mean that the microenvironment with a sufficiently high degree of supersaturation of calcium and phosphate ions is crucial for apatite to nucleate and grow in SBF, while the HA crystalline structure is not critical in the nucleation process, as expected.

Keywords: Hydroxyapatite coatings, plasma spraying, amorphous apatite, apatite nucleation, simulated body fluid

Received 14 March 1996; accepted 8 January 1997

It is generally accepted that plasma-sprayed hydroxyapatite (HA) coating has characteristics in physiological environments that differ from bulk HA ceramics. These differences arise from variations in the material properties of HA coating induced by the plasma-spraying process, during which the HA starting particles are completely melted and then rapidly solidified upon impinging the cool substrate. The as-received coating consists of crystalline and amorphous oxyapatite (OHA), with or without other calcium phosphates such as tricalcium phosphate (TCP) and tetracalcium phosphate monoxide, etc.[1–4]. The typical morphology of the plasma-sprayed coating is composed of pancake-like particles or well-flattened splats and spherical droplets with pores and microcracks[4–6].

Dissolution investigations show that the amorphous phase and other non-apatite calcium phosphates in HA coatings are more soluble than the crystalline calcium apatite[3,7]. The local increase of calcium and phosphate ions, because of the dissolution of the coating, was supposed to be a cause *in vivo* for the increased bone growth into the coating implants[8]. Several immersion experiments indicated that the response of coating *in vitro* is solution sensitive[9–14]: precipitation of the solute ions from simulated physiological fluid occurred on the coating surfaces[9–11], efflorescent crystals formed on the surface of coating in lactic acid solution[12] and in buffered formalin[13], and the only evidence of dissolution of HA coating was observed in Hank's solution[14].

Acellular protein-free simulated body fluid (SBF) is generally adopted to reveal the mechanism of formation of the surface apatite layer on bioactive glasses and glass-ceramics[15,16]. Recently, *in vitro* experiments in SBF were also employed to evaluate the ability of plasma-sprayed[11] and magnetron-sputtered Ca/P

Correspondence to Professor K. de Groot.

coatings[17] to induce an apatite layer. However, the physicochemical processes governing deposition of apatite on the coating surface are still poorly understood.

The present paper is focussed on the nucleation and evolution of the precipitate on the surface of plasma-sprayed HA coating in SBF and how these processes relate to the surface morphology. Compositional and structural analyses are employed to reveal the characteristics of the as-formed layer, with the intention of gaining insight into the material response of the coating to physiological environments.

MATERIALS AND METHODS

HA powder for plasma-spraying was obtained from Merck (Germany). The powder was granulated and sintered in an inert atmosphere. The granules were crushed, milled and sieved to a particle size of less than 45 μm as starting powder. Ti–6Al–4V alloy plates were sand-blasted with Al_2O_3 powder to a surface roughness of 3.5–4.0 μm as a substrate. For cross-section observation, two plates were bound together with screws. Thus, one surface of the substrate was composed of two half-planes so that the fractured section of the coating can be easily obtained simply by separating the two plates. The plasma-spraying process was performed using a Metco MN system (USA). The arc current and voltage were 400–500 A and 40–80 V respectively, with an arc gas of nitrogen. The other plasma-spraying parameters were adopted so that the amorphous and 60% crystalline coatings were prepared[18]. The coatings used in the immersion experiment were as-received and heat-treated at 650°C for 30 min to increase their crystallinity.

SBF was prepared by dissolving reagent grade NaCl, $NaHCO_3$, KCl, $K_2HPO_4 \cdot 6H_2O$, $CaCl_2$ and Na_2SO_4 in distilled water and buffering at physiological pH (7.25) at 36.5°C with trihydroxymethyl aminomethane $[(CH_2OH)_3CNH_2]$ and hydrochloric acid (HCl). It has almost the same ion concentrations as human blood plasma. The coating samples were immersed in SBF-containing vials covered with lids, which were maintained at 36.5°C and subjected to a gentle shaking motion. After different periods of immersion, the coatings were removed from the fluid, rinsed in distilled water and dried at 50°C overnight.

It is known that during the initial periods of wound healing after implantation the environment around the coating is acidic. Therefore, the as-received layer was reimmersed in 0.15 M lactic acid at pH 2.4 and 36.5°C for various periods of time to investigate the stability of the layer in an acidic environment. The heat treatment was also performed on the layer at 750°C for 30 min to increase the crystallinity and to investigate the thermal behaviour.

The surface of samples was sputter-coated with gold for morphological observation by scanning electron microscopy (SEM) or with carbon for elemental analysis by X-ray energy-dispersive spectroscopy (EDS). A few micrograms of the Ca/P layer formed on the coating in SBF were scraped off. This was mixed with KBr and pressed into plates for structural analysis using infrared (IR) spectroscopy.

RESULTS

The as-received coatings show morphologies of well-flattened splats for the amorphous and unmelted particles being embedded in the well-flattened splats for the 60% crystalline material, as shown in *Figure 1*. Pores and a few microcracks can be seen on the surface. After immersion in SBF for 1 h, no evident changes had altered the coating morphology. Three hours later, multiple cracks appeared on the surface of the coating with all surface splats being broken, and the dissolution of the surface seemed moderate and homogeneous, as shown in *Figure 2a*. After 6 h immersion in SBF, the dissolution of the surface became intensive, so that parts of the outer layer of splats dissolved completely, while a few sites of nucleation were seen, especially inside the pores in the close vicinity of dissolved areas, as shown in *Figure 2b*.

Figure 3 shows the morphologies of the coatings immersed in SBF for 12 h. The granular layer appeared on the surface of the recessed regions and pores of the coating. The direction of development of the layer was from the surface of recessed regions to that of

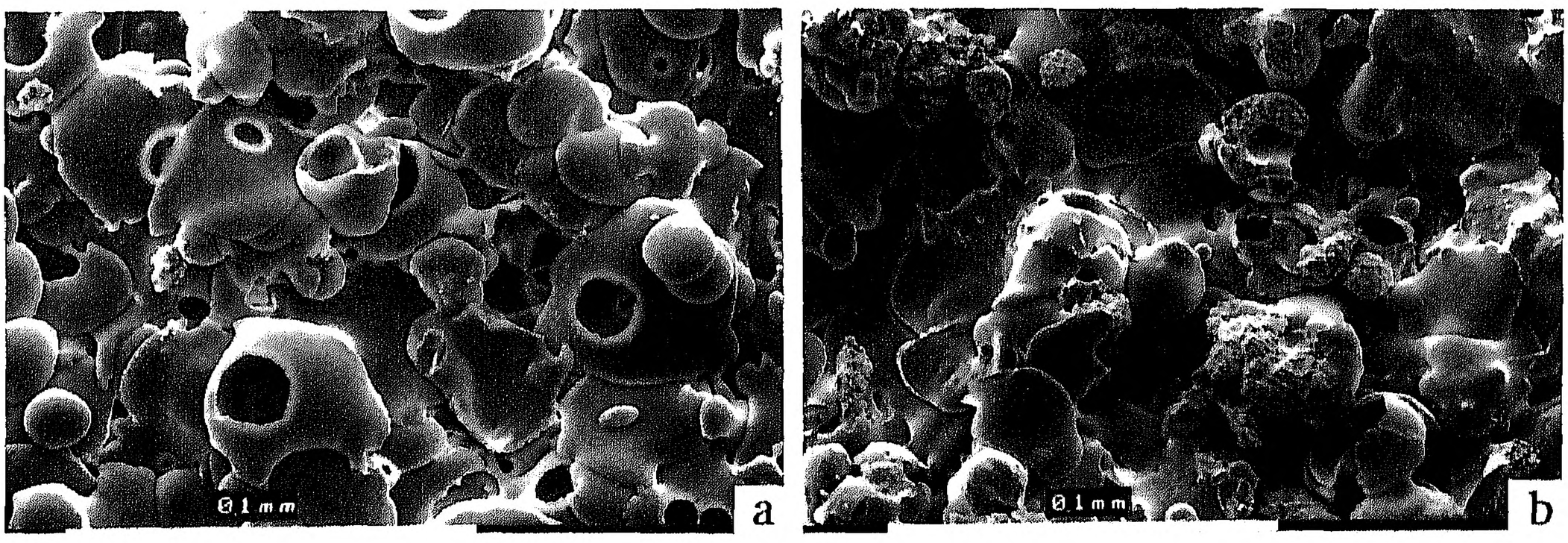

Figure 1 The morphologies of as-received coatings with different crystallinity. **a**, The amorphous coating consists of completely well-flattened splats. **b**, The 60% crystalline coating shows unmelted particles being embedded in well-flattened splats. In both coatings there are microcracks because of the coating process.

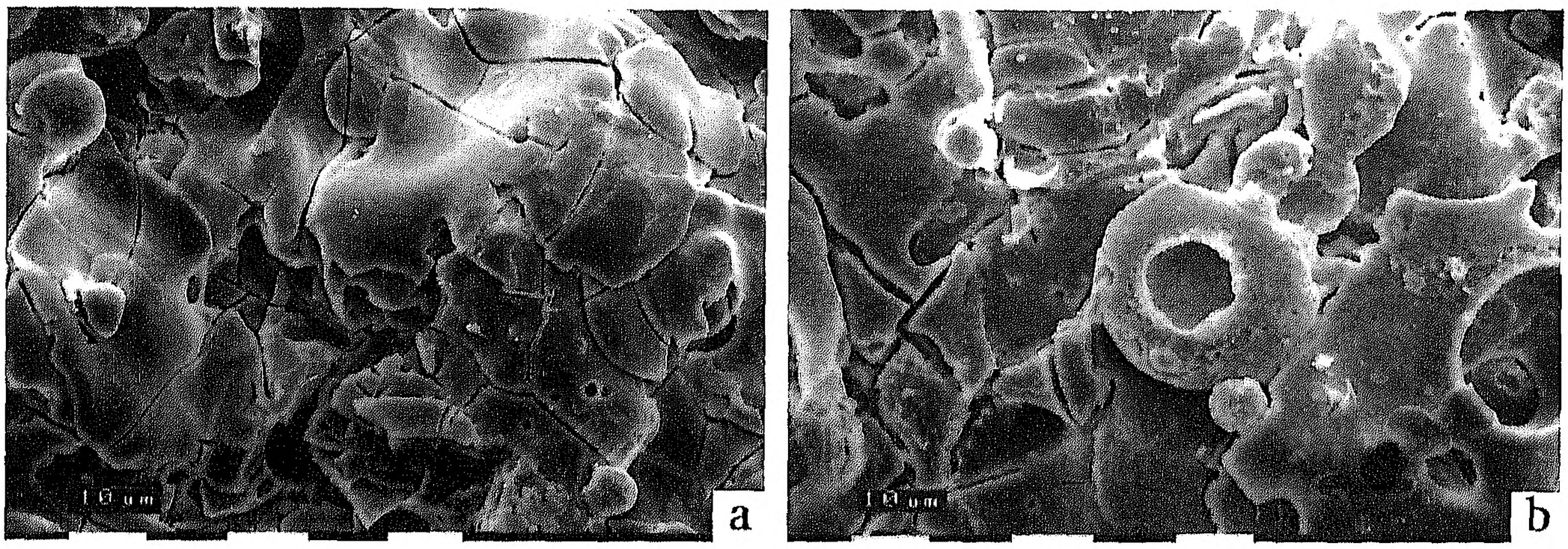

Figure 2 The morphologies of amorphous coatings immersed in SBF for: **a**, 4 h; **b**, 6 h.

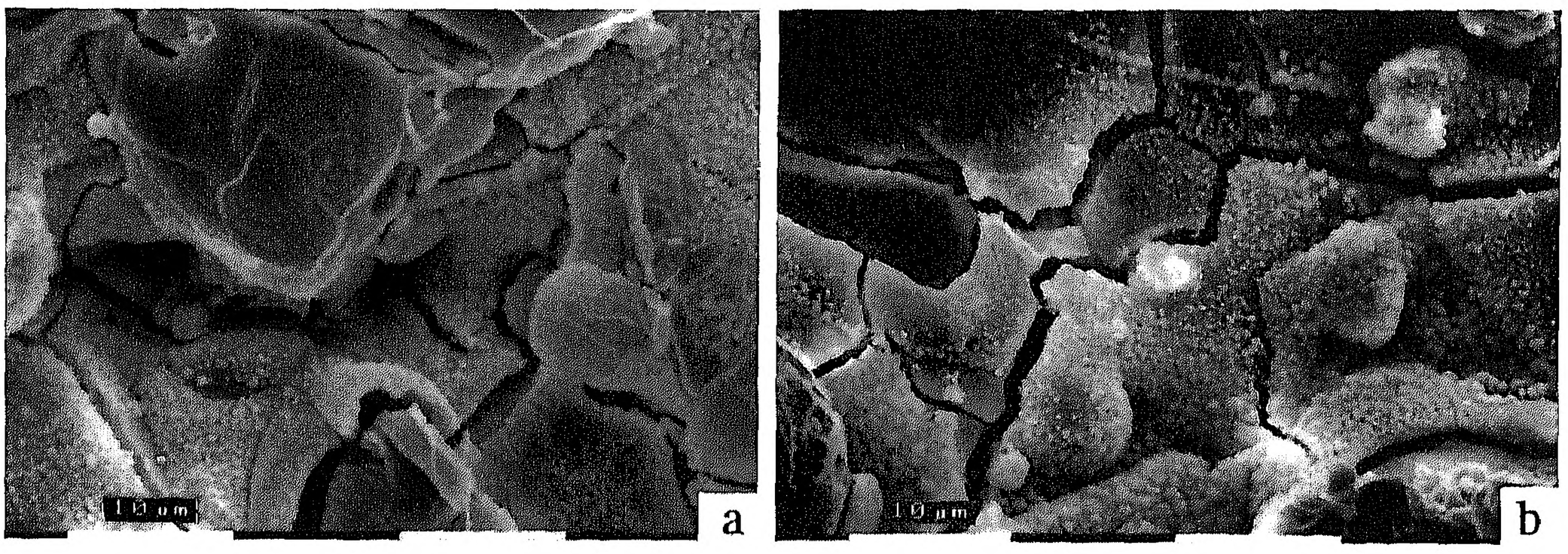

Figure 3 The morphologies of amorphous coatings immersed in SBF for 12 h, showing that the initial deposit is granular. The nucleation began firstly on the surface of recessed regions and pores (**a**), or along microcracks pre-existing in the coating (**b**). The coating exhibited more cracks after drying than during the early period.

protruding regions. The granular line of precipitate formed along the pre-existing microcrack because of the plasma-spraying process. After drying the coating exhibited many more cracks than in the early periods of immersion.

After 24 h immersion in SBF, the surface of the HA coating was completely covered by a dune-like layer with an average mound of 2.5 μm, as shown in *Figure 4*, which changed the original morphology of the as-received coating completely. Moire-like cracks of tortoiseshell character appeared on the newly-formed layer, similar to cracks formed naturally on a dry mud deposit. After 5 days immersion in SBF, the dune-like layer evolved into more smooth hillocks (*Figure 5a*), with a subtle net-like texture consisting of short micro-rods (*Figure 5b*). At later times, the morphology of the layer-covered coating was basically similar to that of coating immersed in SBF for 5 days. The 60% crystalline coating showed the same behaviour in SBF, and developed the same Ca/P layer with the same surface morphology as the amorphous coating.

The layer growing on the coating from SBF is quite dense and homogeneous, which can be seen from the SEM photograph of the cross-section of the coating. *Figure 6* shows the cross-section of fractured coatings immersed in SBF for 5 days and for 28 days. The layer thickness increased with immersion time and bonded tightly to the underlying coating, because there was no obvious interface observed by SEM. After the layer

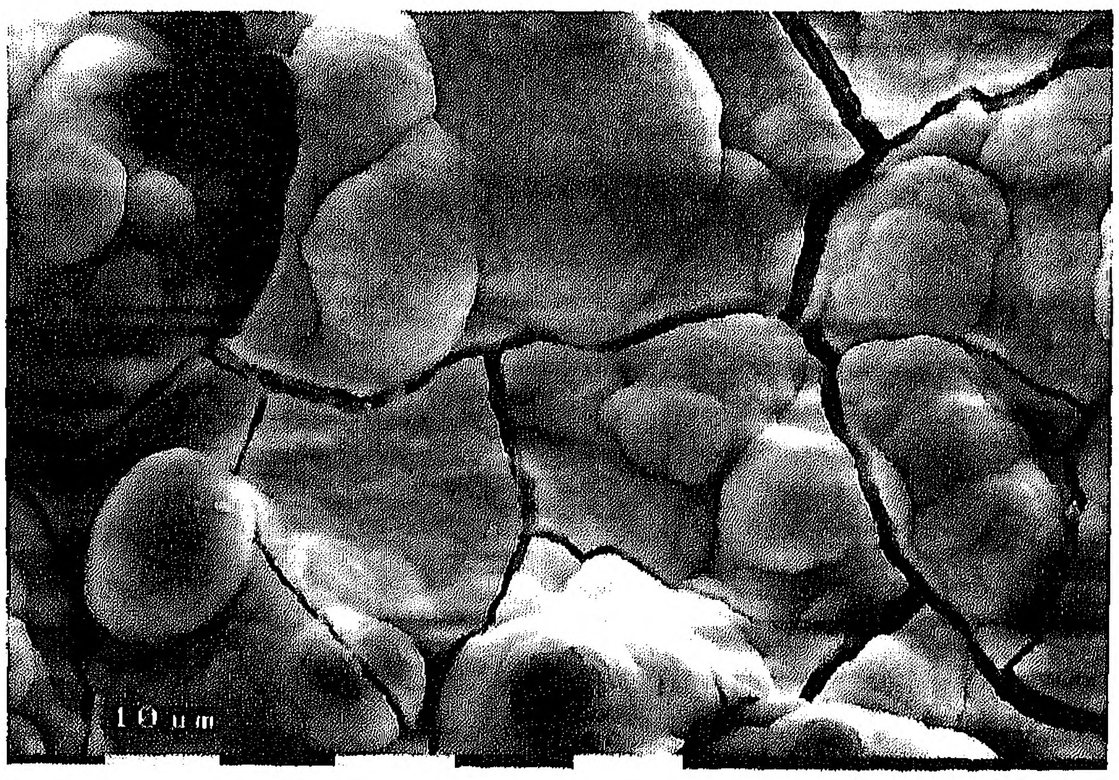

Figure 4 After 24 h immersion, the surface of the coating was completely covered by a dune-like layer with an average mound of 2.5 μm. The original morphology of the as-received coating was completely changed.

immersed in SBF for 28 days was heated at 750°C for 30 min, its colour became quite blue by naked eye observation. It can be recognized that only the layer growing on the coating is blue, while the underlying coating retained its colour when the cross-section was viewed under a light microscope. The heated layer was densified with a smoother and denser surface (*Figure 7a*) and showed no tendency of delamination

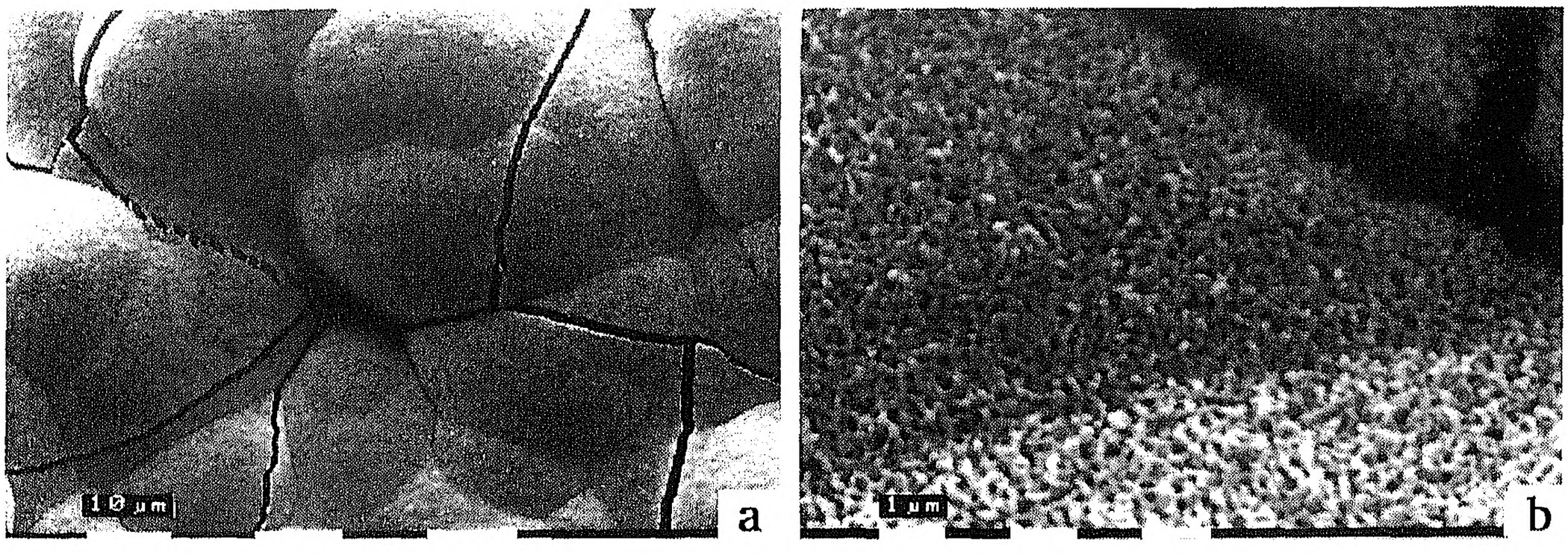

Figure 5 After 5 days immersion, the dune-like layer became more smooth with a hillock of more than 20 μm (**a**). At higher magnification, the surface of the layer shows a net-like structure consisting of short micro-rods (**b**).

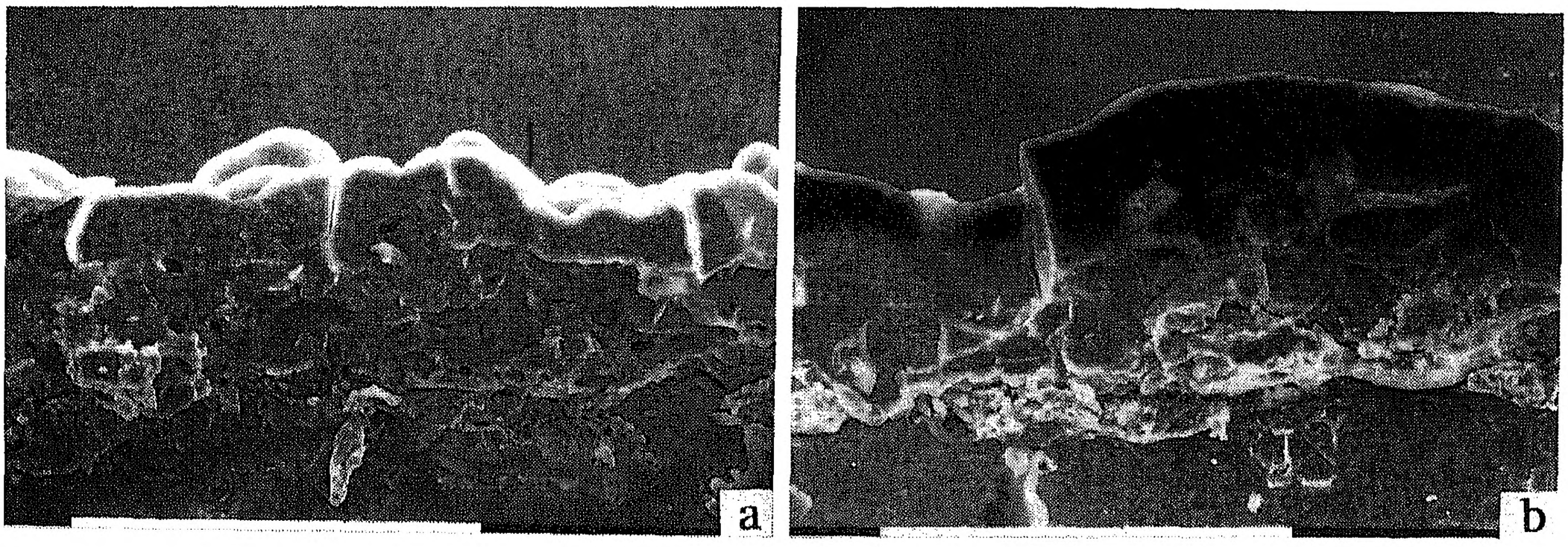

Figure 6 *The morphologies of fractured coatings immersed in SBF for 5 days (**a**) and 28 days (**b**). There is no sharp interface between the layer and the underlying coating.*

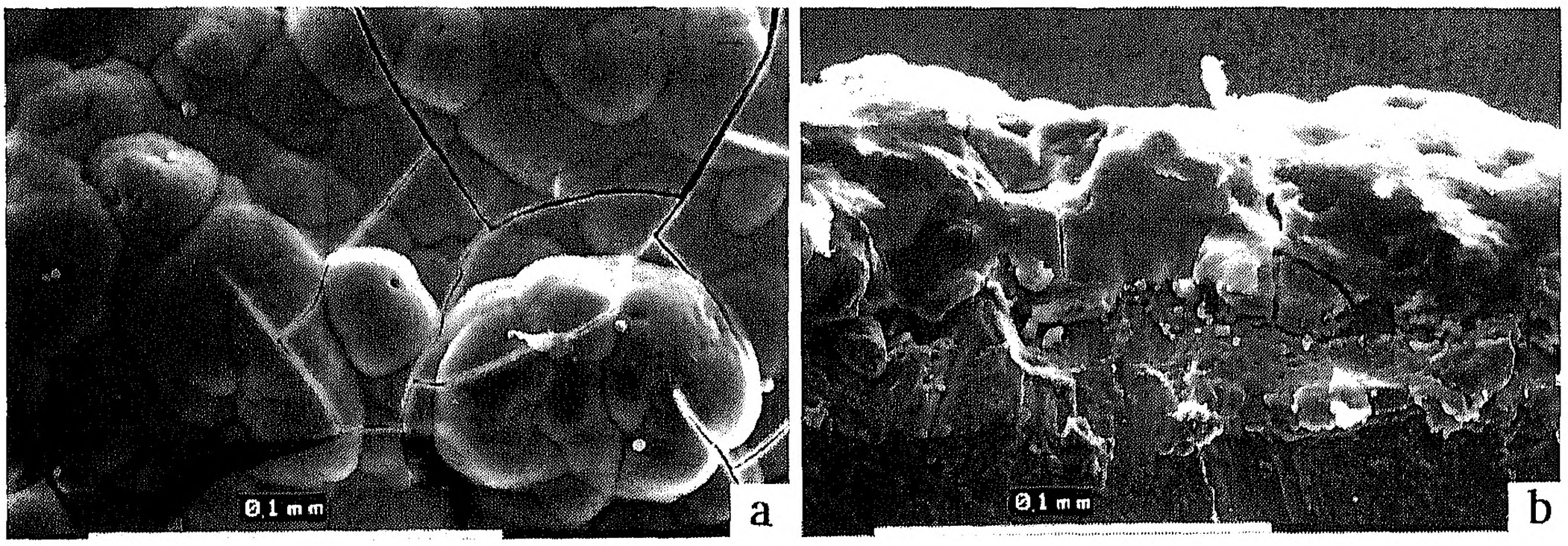

Figure 7 The layer formed in SBF after 28 days immersion was heat-treated at 750°C for 30 min in the atmosphere. The heat treatment made the layer (**a**) densified with a smoother and denser morphology (**b**), but not detached from the underlying coating from the cross-section observation.

from the underlying coating (*Figure 7b*). The morphology of the as-received layer immersed in dilute lactic acid for 1 h showed no evidence of changes in the coating surface.

The EDS spectra of the as-received and heated layers are given in *Figure 8*. The phosphorus content decreased after the layer was heated at high temperature. The quantitative analysis by the standardless mode gave Ca/P ratios of 1.59 and 1.73 for the as-received and heated layers respectively. The existence of magnesium in the layer can clearly be seen. *Figure 9* shows the IR spectra of layers growing on the coating immersed in SBF for 28 days, and then heat-treated at 750°C for 30 min in the atmosphere. The IR spectrum of as-received amorphous coating is also given in *Figure 9c*, showing spectral characteristics of amorphous OHA with ν_1 and ν_3 phosphate bands overlapping and giving a widely-broad peak in the

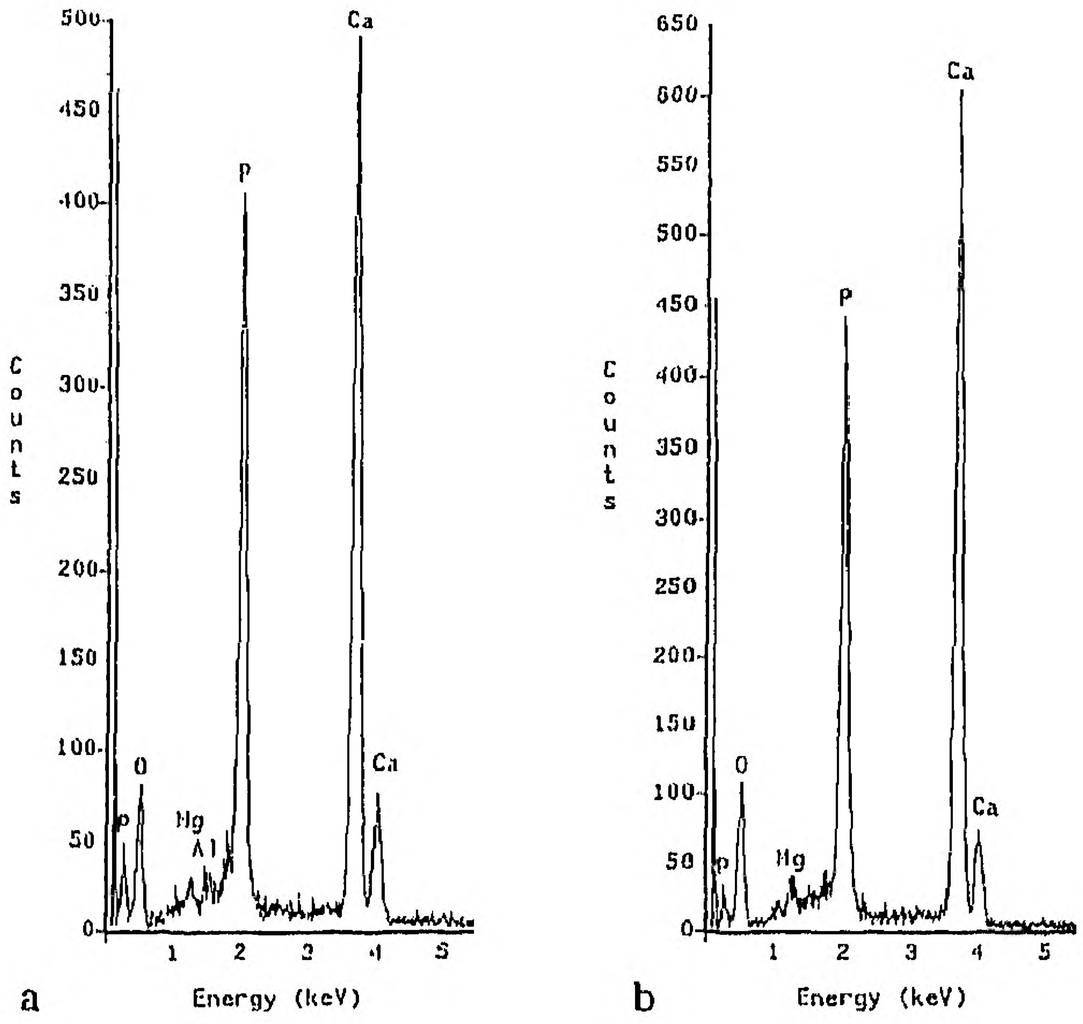

Figure 8 The EDS spectra of the as-received (**a**) and heat-treated (**b**) layers formed on the HA coatings after 28 days immersion.

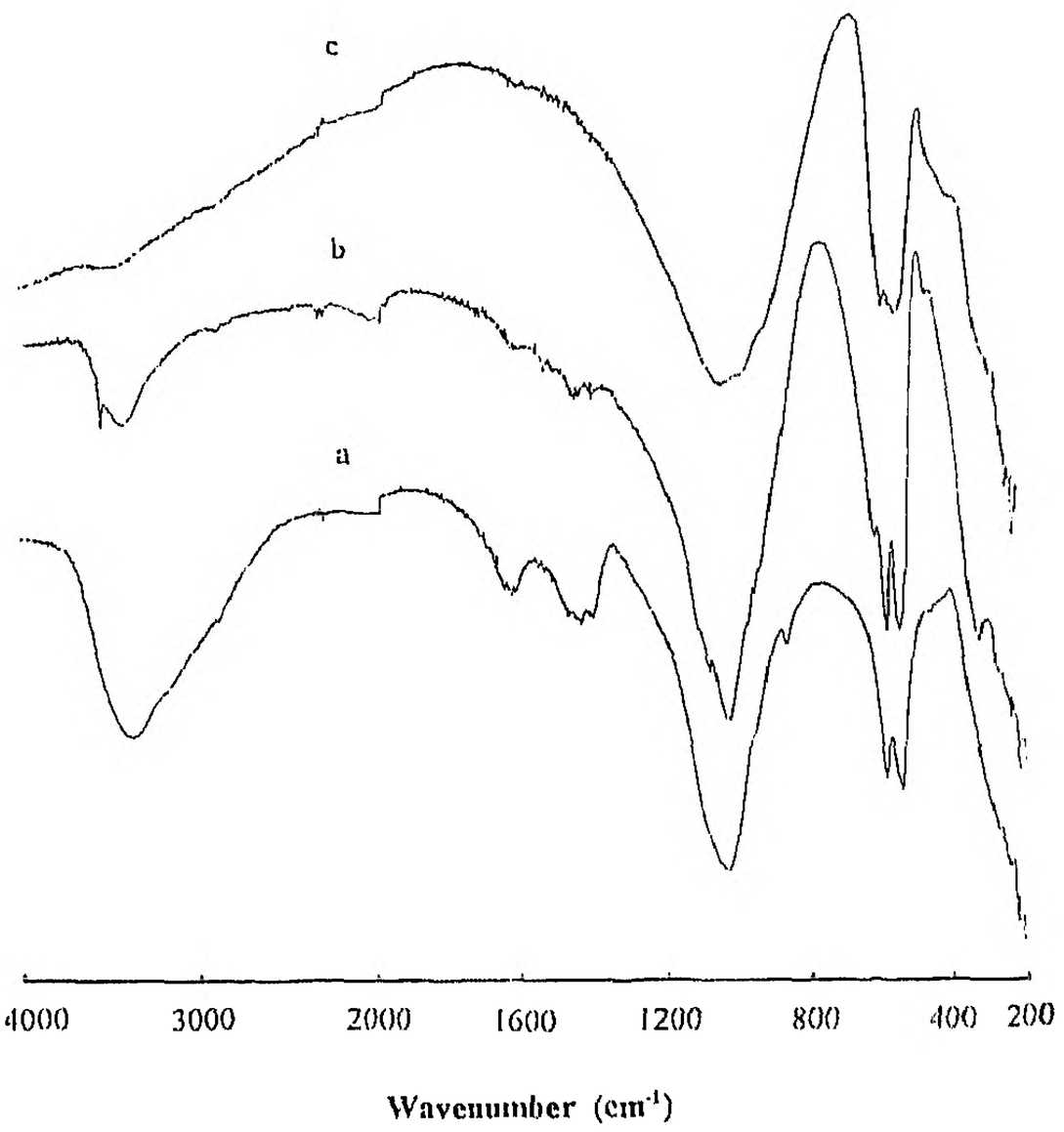

Figure 9 The IR spectra of as-received layers after 28 days immersion (**a**) and then heat-treated at 750°C for 30 min in the atmosphere (**b**), and of the amorphous coating (**c**).

wavenumber interval of 750 to 1500 cm^{-1}. The spectrum of the as-received layer shows that the ν_1 and ν_3 phosphate bands overlap more or less to give a fairly broad peak in the wavenumber interval of 900–1300 cm^{-1}. Water absorbed in the layer was indicated by the broad bands from 3700 to 2500 cm^{-1} and around 1650 cm^{-1}, while no peaks for structural OH groups in the apatite lattice can be seen in the IR spectrum. Bands between 1400 and 1550 cm^{-1} are due to the carbonate IR absorption ν_3. The peak around 870 cm^{-1} is due to the joint contribution of carbonate and HPO_4^{2-} ions. It is known that the HPO_4^{2-} peak disappears after heating at a temperature higher than 600°C, while the carbonate peak is visible in the IR spectrum[19]. The spectrum of the heated layer shows that the peak around 870 cm^{-1} decreases intensively, but was still visible because of the loss of HPO_4^{2-} ions and the maintenance of carbonate.

Moreover, in the spectrum of the heated layer bands are observed at 357, 630 and 345 cm^{-1} due to stretching, librational and translational modes of the OH^- ions in HA; the bands from 900 to 1200 cm^{-1} in the as-received layer become recognizable peaks at 1125, 1090, 1050, 985, 965 and 950 cm^{-1}; there is a shoulder around 545 cm^{-1}. This spectrum has the same typical characteristics as those of the biphasic structures of HA and TCP[20].

The as-received coating heat-treated at 650°C for 30 min recrystallized completely without any change of morphology[21]. The heated coatings were also immersed in SBF for different periods of time. During immersion periods as long as 7 days, the morphology of heated coatings was unchanged by SEM observation: neither surface dissolution nor precipitation was observed. Even after immersion in SBF with two-fold higher concentrations of ions, the nucleation of the Ca/P precipitate was still difficult on the heated coating. There was no morphological change after 24 h immersion. On day 3, a smooth Ca/P layer developed on the heated coatings without the dissolution process (*Figure 10*).

DISCUSSION

According to Kokubo *et al.*[15,16,22,23], the *in vitro* immersion of bioactive materials in SBF is thought to reproduce *in vivo* surface structure changes in materials such as bioactive glass and glass-ceramics. The grown layer is sometimes called a bone-like apatite because of the X-ray diffraction pattern similar to that of bone apatite with broad peaks at 2*θ* angles of HA[24], which indicates a superfine grain of apatite crystallite, and of the carbonate content in the IR spectrum[25]. IR analysis is more sensitive to the group configuration in the apatite lattice, such as the disorder of the phosphate ions from the ideal tetrahedral structure, and the absence of OH^- groups in the lattice.

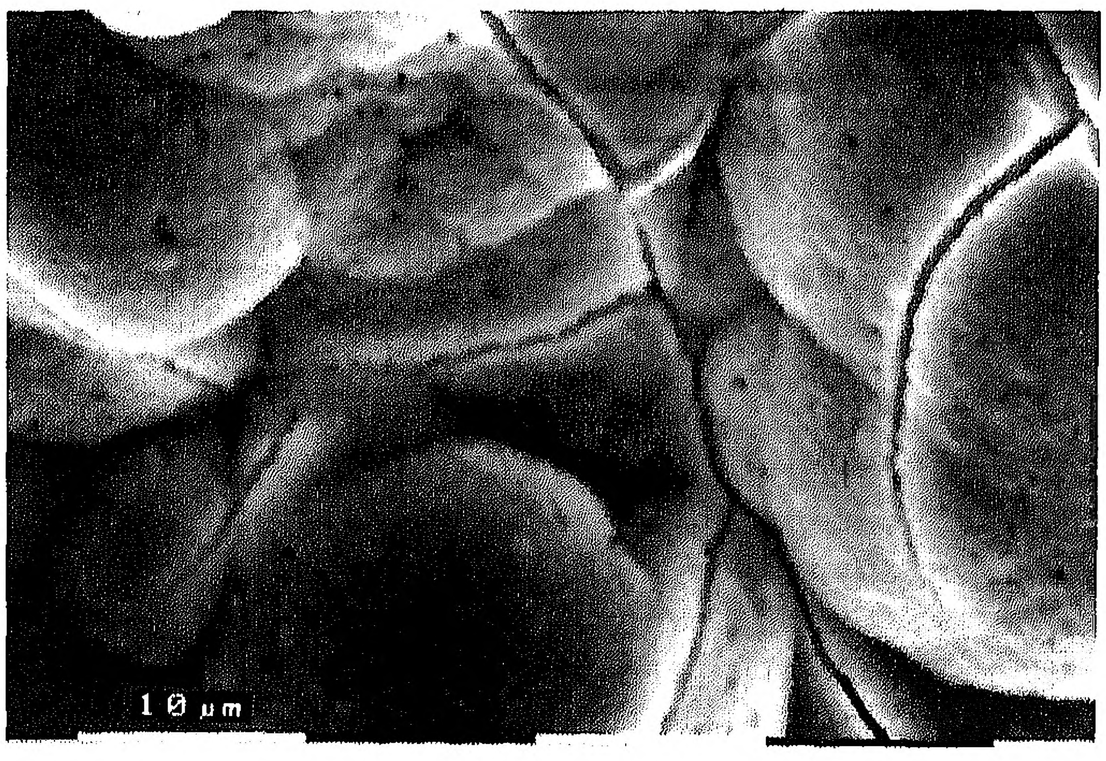

Figure 10 The morphology of the heat-treated coating immersed in SBF with two-fold higher ion concentrations for 3 days shows basically the original form, with a smooth Ca/P layer on the surface.

In the present study, the IR spectrum of the as-received layer (*Figure 9a*) shows the overlap of PO_4 modes at 1090, 1050 and 965 cm^{-1}, indicating the obviation of phosphate ions from the ideal tetrahedral structure. There were broad bands due to absorbed water, without bands for lattice OH^- groups, although the layer was dried at 100°C overnight and following placement in high vacuum of 10^{-5} Torr for 4 h. Therefore, this kind of absorbed water appears to bond to the structure of the layer, i.e. the layer is highly hydrated. There are two possible sites for bonding water: one is the missing OH vacancy[26] and the other the HA surface groups to which the water molecules hydrogen bond[27]. These may cause a shortage of OH groups in the lattice and disturb the perfect structure of the HA lattice. Compared to the needle-like apatite crystals, which give the distinguishing bands of the PO_4 mode at 1090, 1050 and 965 cm^{-1}, and bands of OH groups at 3570, 630 and 340 cm^{-1} [20], the layer is composed of clusters with the imperfect structural unit of apatite, which may be an embryonic form of ideal calcium apatite lattice.

The IR spectrum of the layer heated at 750°C for 30 min exhibits a split of bands of PO_4 mode at 1090, 1050 and 965 cm^{-1} for HA, and at 1125, 985 and 950 cm^{-1} for TCP (*Figure 9b*). It is known that the non-stoichiometric calcium-deficient apatite with Ca/P ratio between 1.67 and 1.33 decomposed into HA and TCP after heat treatment at high temperature[28]. The increase of Ca/P ratio is due to the loss of HPO_4^{2-} ions absorbing on the apatite subjected to heat treatment (*Figure 8*). On the other hand, the quantitative analysis shows that the Ca/P ratio of the layer is less than the value for stoichiometric HA ceramic powder (1.83), even after the layer was sintered at high temperature to release the absorbed HPO_4^{2-} ions (*Figure 8*). A Ca/P ratio greater than 1.67 for the ceramic HA powder comes from the analytical mode used by EDS. Therefore, the as-formed apatite in the layer is calcium deficient and non-stoichiometric.

With the occurrence of decomposition during heating, some chemical and structural processes were in progress, so that the embryonic clusters matured and grew into larger and more perfect crystals. The bonding water may catalyse this maturation during heating. This is suggested from the appearance of OH^- bands at 3570, 630 and 345 cm^{-1} (*Figure 9b*). After heating, the layer consists of biphasic calcium phosphate comprised of HA and TCP with quite perfect crystalline structure. This is also similar to the decomposition of calcium-deficient apatite during heating[20].

Bone apatite contains carbonates, which promote the formation[29] but reduce the size of apatite crystals[30]. Mg^{2+} ions also suppress the growth of apatite[31]. During the *in vitro* immersion of the amorphous coating in SBF, both carbonate and magnesium were incorporated into the clusters of the layer, which may be another cause of the poorly crystalline structural arrangement. In acidic conditions, even well-crystallized HA is soluble under pH 4.2[32], but the apatite layer is stable. This may be because it contains carbonate and is highly hydrated, with the absorbed acidic HPO_4^{2-} ions increasing its acidic properties so that it was stable in dilute lactic acid. During formation of the apatite layer, trace manganese ions from the starting chemicals were incorporated in the clusters and made the layer appear blue after sintering at elevated temperature[33].

Because of the structural similarity between the apatite layer and the underlying coating, the grown layer combined tightly with the coating without an obvious interface (*Figure 6a* and *b*). Heat treatment did nothing to weaken the interface bonding (*Figure 7b*), but might enhance the bonding strength through reaction between the layer and the coating, because of the structural similarity. Therefore, pre-deposition of an apatite layer on HA coatings may be a useful way to improve their stability after the coatings are implanted *in vivo*.

According to classical nucleation theory[34], either of the following two ways can increase the rate of nucleation at a given temperature: increasing the supersaturation or lowering the interfacial energy (σ) at a given supersaturation. Although SBF is supersaturated to apatite[15], the interfacial energy of crystalline HA is not low enough to form nuclei of apatite. This was proved by the fact that no nucleation of apatite occurred on the surface of heated coatings, even after immersion in SBF for 7 days. The stability of the heated coating resulted in almost no dissolution, so that the higher supersaturation for apatite formation cannot be reached. The crystalline structure of HA of the heated coating does not assist in the nucleation of apatite, neither does the complicated morphology of the heated coating. Heat treatment appears to make the amorphous phase in the as-received coating recrystallize into superfine crystallites without change of the coating morphology[21]. During recrystallization, the atoms and ions which obviate from the locations in the ideal apatite structure (*Figure 9c*) return to the stable sites with the lowest crystalline energy. The superfine grains make the polycrystalline surface of the heated coating become almost completely dense, with few intergrain defects. These two effects make the surface of the heated coating, which is composed of well-flattened splats and spherical particles, very stable. Even after 3 days immersion in SBF with two-fold higher ion concentrations, the heat-treated coating basically showed the original morphology, with a very thin layer on the surface (*Figure 10*).

The as-received coating releases both calcium and PO_4 ions by dissolution of the amorphous phase during the first several hours after contact with SBF (*Figure 2*), resulting in an increase of supersaturation. The first nuclei form on the surface of recessed regions and pores or along microcracks of the coating, where the relatively high supersaturation can be maintained steadily (*Figure 3*). The surface roughness due to the dissolution is favourable for the nuclei to anchor. It is suggested that the favourable microenvironment for nucleation of bone-like apatite must be that concentrated with calcium and phosphate ions in the immediate vicinity of the surface upon which the apatite anchors. The morphological evolution of the apatite layer grown from the rough dune-like surface to the smooth hillocks (*Figures 4* and *5*) indicates a polynuclear growth process, during which new nuclei start rapidly before the proceeding layer growth is completed.

There is little difference in response to SBF between the amorphous and 60% crystalline as-received

coatings. The 60% crystalline coatings were received by changing the plasma-spraying parameters so that the starting powder melted partially to increase the crystallinity. After having been subjected to plasma torch, the particles can keep their cores unmelted and encapsulated by the melted outer layer. Upon impinging on the cold substrate, the rapid solidification makes the melted outer layer quench as amorphous phase to form a very thin enamel-like covering on the unmelted cores (*Figure 1b*). The unmelted cores were embedded in the matrix of amorphous phase[35], which resulted in the surfaces of both coatings contacted by SBF being very similar to each other, i.e. having amorphous components. Therefore, it is not surprising that the performance of the as-received coatings, either amorphous or 60% crystalline, is observed to be almost the same in SBF.

The nucleation and growth of the apatite layer resulting from the increased ion concentrations by dissolution will occur only when favourable supersaturation is reached for heterogeneous nucleation. Although the as-received coating was immersed in distilled water for 12 days, there was aggravated dissolution of the surface without growth of a new layer (*Figure 11*). In Ringer's solution, the plasma-sprayed HA coatings showed surface dissolution in the first few weeks and nucleation of spherical crystals at later stages, but no complete film finally formed on the surface[9]. After 3 months incubation in Gomori's buffer, the as-received plasma HA coating showed precipitation, while the corresponding heated coating maintained its surface morphology as observed by SEM[10]. The concentration of calcium ions was almost the same in both solutions with the as-received and heated coatings after 3 months incubation, with precipitation on the surface of the former. Hence, a much higher Ca^{2+} ion concentration was supposed to be maintained near the surface of the as-received coating, where the precipitates finally formed with consumption of calcium and phosphate ions. This did not occur on the heated coating, because the local Ca^{2+} ion concentration was not high enough for precipitates to form. In another immersion experiment in SBF, a layer with the same morphology as that in the present study grew on the three plasma-sprayed Ca/P coatings prepared from different starting HA powders after a 7-day incubation[11]. Furthermore, from all the above discussions it can be suggested that the nucleation and growth of the apatite layer does not distinguish the underlying substrates if supersaturation is favourable.

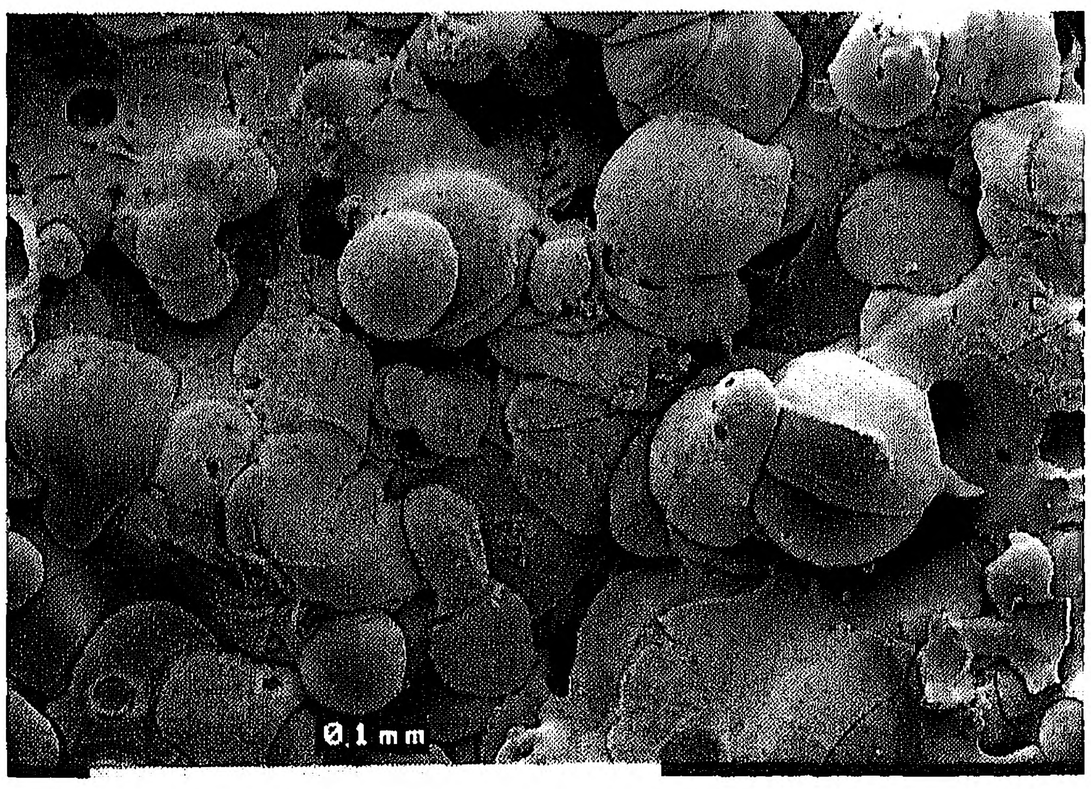

Figure 11 The morphology of the amorphous coating immersed in distilled water for 12 days shows the occurrence of dissolution, but no nucleation.

The ion exchanges between bioactive implants and body fluid are important in establishing bone-bonding at the interface. Partial dissolution of the surface of the implants is necessary for this process. After *in vivo* implantation of the HA ceramics with traces of β-TCP, carbonate apatite nucleated and grew on the ceramic surface through the dissolution effect of the β-TCP component[36,37], which finally led to bone-bonding at the interface between the ceramics and bone tissue. However, the dense polycrystalline HA surface shows little dissolution after long-term implantation *in vivo*[38,39], and the interface bonding to bone seemed more like a micromechanical interlocking of the calcified extracellular matrix by intergranular microvoids on the ceramic surface[40].

The subcutaneous implantation of HA coatings showed that the dissolution of calcium phosphate protected the amorphous coating from further degradation after implantation intervals longer than 6 weeks[41]. However, osseous implantation of the HA coatings showed only resorption of the coatings, without the formation of the surface layer[42]. This may be ascribed to the more acidic microenvironment in osseous sites produced by osteoblasts and activated macrophages[43], in which the amorphous phase dissolved at an accelerated rate.

The dissolution/precipitation process places HA coatings in a dilemma: the stability ensures longevity but the bone-bonding requires dissolution. The apatite layer formed in SBF is stable in acidic solution so that it may protect the HA coating from dissolution in osseous sites with acidic pH, while it enhances fast bone-bonding at the interface. Bone tissue may accept it more easily without a foreign body response because of its similarity to bone apatite. It is well known that a bone-like or carbonate apatite layer plays an important role in establishing the bone-bonding interface between bioactive glasses and living tissues[44].

CONCLUSIONS

The as-received plasma-sprayed HA coating is very reactive in SBF. The dissolution of the amorphous phase and/or other calcium phosphate components in the coating is crucial for the formation of apatite on the surface of recessed regions, pores and along cracks. The apatite layer bonds firmly to the underlying coating, even after it is heat-treated at 750°C for 30 min in air without delamination. The heat-treated plasma-sprayed coating is stable in SBF. When SBF with two-fold higher ion concentration was used, the apatite formed slowly on the surface of the heat-treated coating in 72 h without the dissolution of the surface. The HA structure of the heated coating is not critical for apatite to nucleate in SBF without sufficient dissolution of the coating to increase the local supersaturation of calcium and phosphate ions.

REFERENCES

1. Lemons, J.E., Hydroxyapatite coatings. *Clin. Orthop.*, 1988, **235**, 220–223.
2. Koch, B., Wolke, J.G.C. and de Groot, K., X-ray diffraction studies of plasma-sprayed calcium phosphate coated implants. *J. Biomed. Mater. Res.*, 1990, **24**, 655–667.
3. Radin, S.R. and Ducheyne, P., Plasma spraying induced changes of calcium phosphate ceramic characteristics and the effect on *in vitro* stability. *J. Mater. Sci.: Mater. Med.*, 1992, **3**, 33–42.
4. Zyman, Z., Weng, J., Liu, X., Zhang, X. and Ma, Z., Amorphous phase and morphological structure of hydroxyapatite plasma coatings. *Biomaterials*, 1993, **14**, 225–228.
5. Tayler, M.P., Chandler, P. and Marquis, P.M., The influence of powder morphology on the microstructure of plasma-sprayed hydroxyapatite coatings. In *Bioceramics 6*, ed. P. Ducheyne and D. Christiansen. Butterworth-Heinemann, London, 1993, pp. 185–190.
6. Yang, C.Y., Wang, B.C., Chang, E. and Wu, J.D., The influences of plasma spraying parameters on the characteristics of hydroxyapatite coatings: a quantitative study. *J. Mater. Sci.: Mater. Med.*, 1995, **6**, 249–257.
7. Klein, C.P.A.T., de Blieck-Hogervorst, J.M.A., Wolke, J.G.C. and de Groot, K., A study of solubility and surface features of different calcium phosphate coatings *in vitro* and *in vivo*: a pilot study. In *Ceramics in Substitutive and Reconstructive Surgery*, ed. P. Vincenzini. Elsevier, Amsterdam, 1991, pp. 363–374.
8. Klein, C.P.A.T. and de Groot, K., Implant systems based on bioactive ceramics. In *Osseo-integrated Implants*, Vol. 2: *Implants in Oral and ENT Surgery*, ed. G. Heimke. CRC Press, Boca Raton, FL, 1990, pp. 193–208.
9. Gross, K.A. and Bernd, C.C., *In vitro* testing of plasma-sprayed hydroxyapatite coatings. *J. Mater. Sci.: Mater. Med.*, 1994, **5**, 219–224.
10. Klein, C.P.A.T., Wolke, J.G.C., de Blieck-Hogervorst, J.M.A. and de Groot, K., Features of calcium phosphate plasma-sprayed coatings: an *in vitro* study. *J. Biomed. Mater. Res.*, 1994, **28**, 961–967.
11. Liu, D.M., Chou, H.M. and Wu, J.D., Plasma-sprayed hydroxyapatite coating: effect of different calcium phosphate ceramics. *J. Mater. Sci.: Mater. Med.*, 1994, **5**, 147–153.
12. Weng, J., Liu, X., Zhang, X., Ma, Z., Ji, X. and Zyman, Z., Further studies on the plasma-sprayed amorphous phase in hydroxyapatite coatings and its deamorphization. *Biomaterials*, 1993, **14**, 578–582.
13. Kieswetter, K., Bauer, T.W., Brown, S.A., van Lente, F. and Memitt, K., Alteration of hydroxyapatite coatings exposed to chemicals used in histological fixation. *J. Biomed. Mater. Res.*, 1994, **28**, 281–287.
14. Chern Lin, J.H., Liu, M.L. and Ju, C.P., Morphologic variation in plasma-sprayed hydroxyapatite-bioactive glass composite coatings in Hank's solution. *J. Biomed. Mater. Res.*, 1994, **28**, 723–730.
15. Kokubo, T., Kushitani, H., Ohtsuki, C., Sakka, S. and Yamamuro, T., Chemical reaction of bioactive glass and glass-ceramics with a simulated body fluid. *J. Mater. Sci.: Mater. Med.*, 1992, **1**, 79–83.
16. Li, P., Ohtsuki, C., Kokubo, T. *et al.*, Effects of ions in aqueous media on hydroxyapatite induction by silica gel and its relevance to bioactivity of bioactive glasses and glass/ceramics. *J. Appl. Biomater.*, 1993, **4**, 221–229.
17. Hulshoff, J.E.G., van Dijk, K., van der Waerden, J.P.C.M., Wolke, J.G.C., Ginsel, L.A. and Jansen, J.A., Biological evaluation of the effect of magnetron sputtered Ca/P coatings on osteoblast-like cells *in vitro*. *J. Biomed. Mater. Res.*, 1995, **29**, 967–975.
18. Wolke, J.G.C., de Blieck-Hogervorst, J.M.A., Dhert, W.J.A., Klein, C.P.A.T. and de Groot, K., Studies on thermal spraying of apatite bioceramics. *J. Thermal Spray Technol.*, 1992, **1**, 75–82.
19. Arends, J., Christoffersen, J., Christoffersen, M.R. *et al.*, A calcium hydroxyapatite precipitated from an aqueous solution: an international multimethod analysis. *J. Crystal Growth*, 1987, **84**, 515–532.
20. Li, Y., Klein, C.P.A.T., de Wijn, J., van de Meer, S. and de Groot, K., Shape change and phase transition of needle-like nonstoichiometric apatite crystals. *J. Mater. Sci.: Mater. Med.*, 1994, **5**, 263–268.
21. Zyman, Z., Weng, J., Liu, X., Li, X. and Zhang, X., Phase and structural changes in hydroxyapatite coatings under heat treatment. *Biomaterials*, 1994, **15**, 151–155.
22. Kokubo, T., Kushitani, H., Sakka, S., Kitsugi, T. and Yamamuro, T., Solution able to reproduce *in vivo* surface-structure changes in bioactive glass-ceramics A-W. *J. Biomed. Mater. Res.*, 1990, **24**, 721–734.
23. Kokubo, T., Ito, I., Huang, T. *et al.*, Ca, P-rich layer formed on high-strength bioactive glass-ceramics A-W. *J. Biomed. Mater. Res.*, 1990, **24**, 331–343.
24. Posner, A.S., The mineral of bone. *Clin. Orthop. Rel. Res.*, 1985, **200**, 87–93.
25. Rey, C., Collins, B., Goehl, T., Dickson, I.R. and Glimcher, M.J., The carbonate environment in bone mineral: a resolution-enhanced Fourier transform infrared spectroscopy study. *Calcif. Tiss. Int.*, 1989, **45**, 157–164.
26. Joris, S.J. and Amberg, C.H., The nature of deficiency in nonstoichiometric hydroxyapatite. II. Spectroscopic studies of calcium and strontium hydroxyapatite. *J. Phys. Chem.*, 1971, **75**, 3172–3178.
27. Blumenthal, N.C. and Posner, A.S., Hydroxyapatite: mechanism of formation and properties. *Calcif. Tiss. Res.*, 1973, **13**, 235–243.
28. Rey, C., Freche, M., Heughebaert, M. *et al.*, Apatite chemistry in biomaterial preparation, shaping and biological behaviour. In *Bioceramics 4*, ed. W. Bonfield, G.W. Hastings and K.E. Tanner. Butterworth-Heinemann, London, 1991, pp. 57–64.
29. LeGeros, R.Z., Taheri, M.H., Quirolgico, G.M. and LeGeros, J.P., Formation and stability of apatites: effects of some cationic substituents. In *Proc. 2nd Int. Congr. on Phosphorus Compounds*, Boston, 1980, pp. 89–103.
30. LeGeros, R.Z. and Tung, M.S., Chemical stability of carbonate- and fluoride-containing apatite. *Caries Res.*, 1983, **17**, 419–429.
31. Salimi, M.H., Heughebaert, J.C. and Nancollas, G.H., Crystal growth of calcium phosphates in the presence of magnesium ions. *Langmuir*, 1985, **1**, 119–122.
32. Drissens, F.C., Formation and stability of calcium phosphates in relation to the phase composition of the mineral in calcified tissues. In *Bioceramics of Calcium Phosphate*, ed. K. de Groot. CRC Press, Boca Raton, FL, 1983, p. 17.
33. Li, Y., Klein, C.P.A.T., Zhang, X. and de Groot, K., The relationship between the colour change of hydroxyapatite and the trace element manganese. *Biomaterials*, 1993, **13**, 969–972.
34. Walton, A.G., *The Formation and Properties of Precipitates*. Interscience, New York, 1967.
35. Chen, J., Wolke, J.G.C. and de Groot, K., Microstructure and crystallinity in hydroxyapatite coatings. *Biomaterials*, 1994, **15**, 396–399.
36. Heughebaert, M., LeGeros, R.Z., Gineste, M., Guilhem,

A. and Bonel, G., Physicochemical characterization of deposits associated with HA ceramics implanted in nonosseous sites. *J. Biomed. Mater. Res.: Appl. Biomater.*, 1988, **22**, 257–268.
37. Daculsi, G., LeGeros, R. Z., Heughebaert, M. and Barbieux, I., Formation of carbonate-apatite crystals after implantation of calcium phosphate ceramics. *Calcif. Tiss. Int.*, 1990, **46**, 20–27.
38. Denissen, H. W., Walk, W., Veldhuis, A. A. H. and van der Hooff, A., Eleven year study of hydroxyapatite implants. *J. Prosthet. Dent.*, 1989, **61**, 706–712.
39. Gumaer, K. I., Sherer, A. D., Slighter, R. G., Rothstein, S. S. and Drobeck, H. D., Tissue response in dogs to dense HA implantation in the femur. *J. Oral Maxillofac. Surg.*, 1986, **44**, 618–627.
40. Davies, J. E., Pilliar, R. M., Smith, D. C. and Chernechy, R., Bone interfaces with retrieved alumina and hydroxyapatite ceramics. In *Biomaterials 4*, ed. W. Bonfield, G. W. Hastings and K. E. Tanner. Butterworth-Heinemann, London, 1991, pp. 119–204.
41. van Blitterswijk, C. A., Bovell, Y. P., Flach, J., Leenders, H., Brink, I. V. D. and de Bruijn, J., Variations in hydroxyapatite crystallinity: effects on interface reactions. In *Hydroxyapatite Coated Hip and Knee Arthroplasty*, ed. J. A. Epinette and R. G. T. Geesink. Expansion Scientifique Française, Paris, 1995, pp. 33–40.
42. Klein, C. P. A. T., Wolke, J. G. C., de Blieck-Hogervorst, J. M. A. and de Groot, K., Calcium phosphate plasma-sprayed coatings and their stability: an *in vivo* study. *J. Biomed. Mater. Res.*, 1994, **28**, 909–917.
43. Silver, I. A., Murrills, R. J. and Etherington, D. J., Microelectrode studies on the acid microenvironment beneath adherent macrophages and osteoclasts. *Exp. Cell Res.*, 1988, **175**, 266–276.
44. Hench, L. L., Bioceramics, from concept to clinic. *J. Am. Ceram. Soc.*, 1991, **74**, 1482–1510.